Radiometric Characterization of IKONOS Multispectral Imagery

Mary Pagnutti[1], Robert E. Ryan[2], Michelle Kelly[3], and Kara Holekamp[4], Lockheed Martin Space Operations – Stennis Programs, Stennis Space Center, Mississippi 39529, USA

Vicki Zanoni[5], NASA Earth Science Applications Directorate, Stennis Space Center, Mississippi 39529, USA

Kurtis Thome[6], Remote Sensing Group, Optical Sciences Center, University of Arizona, Tucson, Arizona 85721, USA

Stephen Schiller[7], Physics Department, South Dakota State University, Brookings, South Dakota 57007, USA

---

[1] Corresponding author. Tel.: +1-228-688-2135; fax: 228-688-7694; e-mail: Mary.Pagnutti@ssc.nasa.gov

[2] Tel.: Fax: 228-688-7694; e-mail: Robert.Ryan@ssc.nasa.gov

[3] e-mail: mmkelly@nppd.com

[4] Fax: 228-688-7694; e-mail: Kara.Holekamp@ssc.nasa.gov

[5] Fax: 228-688-7455; e-mail: Vicki.Zanoni@ssc.nasa.gov

[6] Fax: 520-621-8292; e-mail: kurt.thome@opt-sci.arizona.edu

[7] e-mail: Stephen_J_Schiller@west.raytheon.com

Abstract

A radiometric characterization of Space Imaging's IKONOS 4-m multispectral imagery has been performed by a National Aeronautics and Space Administration (NASA) funded team from the John C. Stennis Space Center (SSC), the University of Arizona Remote Sensing Group (UARSG), and South Dakota State University (SDSU). Both intrinsic radiometry and the effects of Space Imaging processing on radiometry were investigated. Relative radiometry was examined with uniform Antarctic and Saharan sites. Absolute radiometric calibration was performed using reflectance-based vicarious calibration methods on several uniform sites imaged by IKONOS, coincident with ground-based surface and atmospheric measurements. Ground-based data and the IKONOS spectral response function served as input to radiative transfer codes to generate a Top-of-Atmosphere radiance estimate. Calibration coefficients derived from each vicarious calibration were combined to generate an IKONOS radiometric gain coefficient for each multispectral band assuming a linear response over the full dynamic range of the instrument. These calibration coefficients were made available to Space Imaging, which subsequently adopted them by updating its initial set of calibration coefficients. IKONOS imagery procured through the NASA Scientific Data Purchase program is processed with or without a Modulation Transfer Function Compensation kernel. The radiometric effects of this kernel on various scene types was also investigated. All imagery characterized was procured through the NASA Scientific Data Purchase program.

Keywords

Remote Sensing, Imagery, Ground Truth, Calibration

1. Introduction

The National Aeronautics and Space Administration (NASA) Earth Science Enterprise (ESE) is evaluating a new way of obtaining remote sensing datasets for its research objectives through the Scientific Data Purchase (SDP) program. As a pathfinder for a new way of doing business, NASA purchases data without the up-front investment, as required with a traditional approach where a remote sensing system is built and operated by the U.S. government. The NASA Stennis Space Center (SSC) Earth Science Applications Directorate (ESAD), which manages the SDP, administers five contracts with commercial companies that were selected through a NASA competitive solicitation process. Earth Satellite Corporation (EarthSat), Space Imaging LLC, EarthWatch Inc., Positive Systems Inc., and AstroVision were originally awarded a NASA contract to provide remotely sensed image products. Image products are also being procured from DigitalGlobe with additional data purchase funds. ESAD is also responsible for verification and validation of products delivered under the SDP. For more detailed descriptions of the SDP project and of each of the commercial products, access the ESAD Web page at http://www.esad.ssc.nasa.gov/datapurchase/dbmain.asp.

The IKONOS satellite, owned and operated by Space Imaging, LLC, of Thornton, Colorado, is the first of a new class of commercial remote sensing satellites with unprecedented spatial resolution (4-m multispectral ground sample distance (GSD) and 1-m panchromatic GSD). The U.S. government is prohibited from competing with U.S. private industry and thus cannot provide a similar service. Therefore, several federal government agencies, including NASA, the National Imagery and Mapping Agency (NIMA), the U. S. Geological Survey

(USGS), and the National Oceanic and Atmospheric Administration (NOAA), as well as state and local governments, all must purchase commercial imagery for a wide range of applications.

The unique imagery available from IKONOS and other high-spatial-resolution systems becoming available has great potential for U.S. government-sponsored research. IKONOS datasets open new opportunities for virtual ground truthing by validating conclusions derived from the government's coarser spatial-resolution systems. For the first time, phenomena inferred by spectral processing of coarse-resolution data can be validated using this high-spatial-resolution data. In addition, other Earth science research can now be supported by data with significantly greater fidelity. IKONOS can resolve features in scenes that Landsat 7, with its 30-m GSD and 8-bit dynamic range, cannot resolve. In addition, spatial structure of dark scenes, such as dense forest canopies, can now be investigated from space-derived IKONOS data (Bauer and Sawaya, 2001). IKONOS radiometric calibration and its associated accuracy are critical for many of these studies, particularly when comparing data from other systems, performing atmospheric correction, or estimating various vegetative indices (Justice et al., 1991).

Commercial data products must be highly characterized to be useful to NASA's broad science community and to other government users. Because commercial and science requirements often differ, commercial providers do not necessarily characterize systems in the manner that NASA researchers desire or need. Commercial imagery is typically highly processed, being radiometrically and geometrically corrected and possibly sharpened before it is delivered. This is a new paradigm for the NASA science community – a community historically having significant insight into sensor design and operation. This new way of doing business, therefore,

requires independent data characterization and a thorough understanding of how product processing impacts the imagery.

The primary objective of this investigation was to perform relative and absolute radiometric assessments of IKONOS 4-m multispectral imagery. Three independent groups performed vicarious calibrations: NASA SSC, the University of Arizona Remote Sensing Group (UARSG), and South Dakota State University (SDSU). A detailed discussion of each group's vicarious calibration is presented. Each group used some variant of a reflectance-based vicarious radiometric characterization method in which surface and atmospheric measurements taken at the time of the satellite overpass were used to predict Top-Of-Atmosphere (TOA) radiance. These results were combined to derive an IKONOS radiometric gain coefficient for each multispectral band assuming a linear response over the full dynamic range of the IKONOS multispectral imagery. The gain coefficients were then compared to those provided by Space Imaging.

A secondary objective of this investigation was to evaluate the radiometric effects of image enhancements routinely provided by Space Imaging to its customers. Space Imaging's commercial Carterra^{TM} product is processed with a Modulation Transfer Function Compensation (MTFC) function. This imagery is visually superior to nonenhanced imagery but is subject to some artifacts, such as ringing near high-contrast edges. MTFC is an edge-sharpening technique that is used to restore partially, image degradation due to finite detector size, optical aberrations, motion, diffraction, and electronic effects. It has been used to sharpen Cathode Ray Tube displays, and the intelligence community has used MTFC to improve manmade object recognition (Holst, 1995; Leachtenauer et al., 1997). MTFC can take many forms and is usually implemented in software.

During the initial phase of the SDP, imagery with MTFC applied (MTFC-On) was the only option provided by Space Imaging. Therefore, a significant portion of the vicarious calibration imagery being analyzed was with MTFC-On. Several months into the contract, Space Imaging provided an option for NASA to procure MTFC-Off imagery. The fundamental question of whether MTFC should be applied to data being procured under the NASA SDP arose. It should be noted that Space Imaging's standard Carterra™ products are typically provided with MTFC-On and NASA does not necessarily want to procure a nonstandard product, since researchers in the future may procure imagery directly from Space Imaging. However, if MTFC significantly impacts the results of some scientific investigation, for better or worse, the form of the imagery that most benefits the researcher should be procured. Therefore, MTFC effects on various scene types were investigated to provide some guidance as to when this type of processing is appropriate.

2. IKONOS Satellite Background

The IKONOS satellite was built by Lockheed Martin and launched on an Athena II rocket on September 24, 1999, from Vandenburg, California. The satellite is operated in a sun-synchronous orbit at a 681-km altitude and a 98.1-degree inclination angle. The orbit has a descending node with an equatorial crossing of 10:30 a.m. local time. The satellite is extremely agile, with both in-track and cross-track body pointing.

The IKONOS camera was built by Eastman Kodak and consists of an *f*/14.3 10-m focal length, off-axis, three-mirror anastigmatic telescope and silicon CCD detector system. The IKONOS camera is a pushbroom sensor with a panchromatic band and four multispectral bands. There are 13,500 panchromatic detectors with 12-micron pitch and 3,375 multispectral detectors

with 48-micron pitch. At nadir, the panchromatic GSD is 0.82 m and the multispectral GSD is 3.28 m. At 40 degrees latitude, the revisit time is 2.9 days for 1-m resolution panchromatic imagery. Three separate silicon CCD arrays are used to cover the full swath. The panchromatic band exposure is controlled with time delay integration (TDI), while the multispectral bands have a fixed integration time. The multispectral bandpasses are similar to the first four Landsat Thematic Mapper (TM) bands and are shown in Figure 1. The near-infrared (NIR) band is a slightly modified Landsat TM band that minimizes atmospheric water absorption. Dielectric stack interference filters and the inherent detector response define the multispectral response. The Digital Number (DN) dynamic range of the system is approximately 1800 with 11 bits quantization. The data are compressed onboard from 11 bits per pixel to 2.6 bits per pixel for data transmission and are restored on the ground. The effects of these compressions appear to be minimal (Brower et al., 2000); however, small effects are observed for low dynamic range scenes.

3. NASA SDP IKONOS Data Products

The NASA SDP provides several types of IKONOS data products to the ESE and to affiliated researchers. NASA procures only products that are both radiometrically and geometrically corrected, similar to the Space Imaging commercial Carterra™ products. The IKONOS SDP imagery is divided into Original and Master classes. Original imagery is georectified, and Master imagery is orthorectified. All data are projected to a Universal Transverse Mercator (UTM)/World Geodetic System of 1984 (WGS84) Datum. Both Original and Master imagery can be ordered through the SDP with either Standard or Precision geometric accuracy. Standard products are georectified without the use of surveyed ground control points

while Precision products utilize ground control points. Most of the radiometric analysis discussed in this paper was performed on Standard Original imagery. Raw intrinsic panchromatic and multispectral imagery is spatially resampled to 1 m and 4 m, respectively, and georeferenced using either a cubic convolution or a nearest-neighbor interpolation algorithm. Off-nadir viewing is typically limited to 26 degrees off-axis for the NASA SDP products to guarantee 1-m or better intrinsic data. In addition, IKONOS imagery is processed with or without Modulation Transfer Function Compensation.

The absolute radiometric accuracy of the IKONOS data product is specified to be better than 10 percent, and the relative radiometric accuracy of the product is specified to be better than 5 percent. Absolute radiometric values are defined in terms of the National Institute of Standards and Technology (NIST) or of another traceable source. In the context of this paper, relative radiometric characterizations compare radiometry between pixels or arrays observing the same radiance. In a pushbroom system, such as IKONOS, each pixel in the array must be corrected for gain and offset variation. In addition to inherent detector-to-detector differences, vignetting and spatial filter variations must also be corrected. Space Imaging precorrects each pixel so a single radiometric coefficient can be applied to all pixel DNs within each band to determine the radiance value, which significantly simplifies the calibration for the user.

4. Relative Radiometric Accuracy Assessment

NASA performed a relative (pixel-to-pixel within a single band) radiometric accuracy assessment using large uniform scenes. Several sites were used, including extremely uniform Antarctic ice sheets from the SDP archive and selected uniform Saharan sites. The Saharan sites were identified by searching through EarthSat Landsat 5 TM imagery purchased through the

SDP. The 30-meter GSD Landsat images were evaluated, and extremely uniform areas within these images were chosen for this investigation (Hilbert et al., 2002). Both the Antarctic and Saharan sites were extremely uniform, so slight differences between the three IKONOS focal plane array calibrations were observed in the imagery. Previous studies have used Advanced Very High Resolution Radiometer (AVHRR) and MeteoSat to identify uniform sites (Kaufman and Holben, 1993). Sites identified with the large kilometer class GSD of these systems, however, were not uniform enough at the 4-m class GSD IKONOS scale and could not be used.

For pushbroom systems such as IKONOS, variations between detectors appear in the in-track direction of scanning. Bad detectors manifest themselves as dark or white lines in the in-track direction on the imagery, and slight differences in calibration between arrays show up as banding. Figure 2 shows the blue multispectral IKONOS band for one of the uniform Saharan scenes located in Libya. This image has a DN range of 590 – 765 and has been stretched to see the in-track banding resulting from the three separate IKONOS detector arrays. The figure also shows a thin white vertical line, indicating a faulty detector.

In general, variations within a single detector array are not easily observed because image processing attempts to minimize deleterious image artifacts. Therefore, to better visualize array and detector defects, columns of pixels in the image were summed and normalized. The summing process, in essence, increases the signal-to-noise ratio and amplifies any image defects. Figure 3 shows a cross sectional plot of this summing, indicating that the differences between arrays (banding) are less than 1.5 percent for each band, which is well within the NASA SDP IKONOS relative radiometric accuracy specification. The plot also shows that a few pixels have DN values slightly less than their adjacent pixels. This is most clearly seen in the blue band on

the first detector array. The single white stripe shown in Figure 2 appears as a single spike in the cross sectional summation plot (Figure 3), and the array transitions appear as step discontinuities. Similar results were obtained with the other Saharan and Antarctic scenes. Overall, the imagery is well corrected, and our analysis illustrates how Space Imaging can provide a single calibration coefficient instead of a set of coefficients (one for each detector).

5. Absolute Radiometric Accuracy Assessment

NASA SSC, the UARSG, and SDSU all use a reflectance-based vicarious calibration method to evaluate the absolute IKONOS multispectral imagery radiometry (Dinguirard and Slater, 1999; Kaufman and Holben, 1993; Meygret et al., 2000; Slater et al., 1987; Slater et al., 1994; Slater et al., 1996; Thome et al., 1993). This method involves imaging a relatively uniform area of interest coincident with taking ground-based measurements. TOA spectral radiance is estimated from ground reflectance, atmospheric pressure, water, and aerosol profile measurements. The sensor spectral response function, provided by Space Imaging from laboratory measurements, is used to estimate the measured in-band radiance. The sites used in this investigation are listed in Table 1. This table summarizes the location, collection dates and times, as well as satellite elevation and azimuth angle. Each team's approach and results are discussed, and a compilation of all the measurements is presented.

6. NASA SSC Vicarious Characterization

Lunar Lake playa in Nevada was chosen for the NASA SSC IKONOS vicarious characterization due to its high surface albedo, which exceeds 30 percent for all four IKONOS multispectral bands, and its location in a high-altitude desert region approximately 1.7 km above sea level. The site receives little precipitation and has a high percentage of cloud-free days. The

playa is actually a dry lakebed consisting of hard packed clay, which is uniform over a large area. The UARSG has found, based on previous measurements, that the surface of the playa is approximately lambertian at viewing angles up to 30 degrees off nadir. NASA scientists routinely utilize the Lunar Lake site for radiometric calibration of airborne and spaceborne sensors.

The IKONOS image taken on June 7, 2000 is shown in Figure 4. The zoomed inset shows the area of playa used by NASA SSC. The NASA SSC site is marked by four Tracer Inc., 8x8-meter tarps provided by Boeing Corporation, which were used for other vicarious calibrations being performed at the same time. The 8x8-meter tarps are too small for the IKONOS 4-m GSD multispectral radiometric characterization other than to serve as fiducial markers. Each tarp was GPS surveyed to a few meters accuracy and can be easily found in the georeferenced IKONOS image. The vans that were used to arrive at the playa can be seen to the left of the tarps in the image. It is interesting to note that the van tire tracks are also visible from space. The reflectance of the tire tracks is higher than the rest of the playa by a few percent, since the surface cracks, naturally found throughout the playa, are compressed and filled in by the weight of the vans as they drove over the playa.

The NASA SSC ground reflectance measurements of Lunar Lake playa were taken on three separate transect lines using two hand-held Analytical Spectral Device FieldSpec® Full Range spectroradiometers (ASDs). These are commercially available spectroradiometers, which have a full width half maximum of 3 nm in the 350 to 1000-nm spectral range and a full width half maximum of 10 nm in the 1000 to 2500-nm spectral range. The output from the spectroradiometers is interpolated within the ASD software to report data at 1-nm sampling

across the entire spectral range. Both ASDs were optimized at the start of each transect line, before any measurements were taken.

Each transect line was divided into 11 different discrete ASD measurement stations. Reflectance measurements along two of the transect lines were entirely of playa ground surface with sampling distances of 12.5 m between measurement stations. Ground reflectance measurements along the third line were comprised of both playa ground surface and tarps. A distance of 12.5 m (approximately 3 pixels) existed between each measurement station and 25 m (approximately 6 pixels) between the tarp center points. Analysis has shown that tarp effects on the measurement are minimal at 3 pixels away from the edge. Before each station measurement, a 99 percent reflectance Labsphere Spectralon® panel measurement was taken to generate reflectance values. The ASD spectroradiometer instruments were programmed to take 250 spectra (10 measurements with 25 spectra averages) at each station. In addition, the ASDs were carefully moved back and forth while measuring the surface at each measurement station to increase the spatial averaging at each location. Dark current readings were also taken at each station with one of the ASDs.

Vicarious calibrations were performed at Lunar Lake playa on two separate days, June 7 and June 10, 2000. There was little to no cloud cover on either day. The NASA SSC team fielded a Yankee Environmental Systems Multi-Filter Rotating Shadowband Radiometer (MFRSR) at Lunar Lake but it failed to record data due to a memory card failure. The UARSG team, however, provided solar radiometer (Ehsani, Reagan, and Erxleben, 1998) measurements taken at Railroad Valley playa on June 7. Railroad Valley playa is approximately 30 km northeast of Lunar Lake playa. The UARSG acquired solar radiometer data at Lunar Lake on June 10. ASD

measurements were taken along two transect lines (playa only and tarp/playa transect) on June 7 and along all three lines on June 10. A radiosonde balloon was also launched prior to each IKONOS overpass. IKONOS acquired data on June 7 at 18:15 Coordinated Universal Time (UTC) at an elevation angle of 71.0 degrees and an azimuth angle of 157.9 degrees and again on June 10 at 18:23 UTC at an elevation angle of 73.0 degrees and an azimuth angle of 350.7 degrees as shown in Figure 5.

The NASA SSC TOA radiance analysis approach is a two-step process. The first step creates a representative atmosphere to accurately estimate aerosol and molecular constituents for radiative transfer calculations at the time of the satellite collection. The second step uses the representative atmosphere, location, time, sensor viewing geometry, sensor spectral response, and reflectance data to estimate TOA radiance.

The representative atmosphere was obtained by using the calibrated sun photometer optical depth measurements at the time of the satellite acquisition along with radiosonde data, site latitude and longitude and time of acquisition. The radiosonde data were used to create input atmospheric layers for MODTRAN (Berk et al., 1999) radiative transport calculations. The pressure, temperature, and humidity radiosonde profile was used to estimate Rayleigh scattering and water vapor absorption. The amount of aerosol in the atmosphere was estimated by varying the surface range of the boundary layer in MODTRAN until the predicted extinction at each sun photometer channel best agrees in a least squares sense with the sun photometer measurements. For this analysis, a mid-latitude summer aerosol was used.

For June 10, the optimal surface range for the boundary layer was found to be 70 km. Typical surface range values often exceed 100 km, but a few thin cirrus clouds were noted on

that day at Lunar Lake. Comparisons between the solar radiometer transmission measurements and MODTRAN predictions are shown in Figure 6. As can be seen, there is excellent agreement between the solar radiometer transmission measurements and the MODTRAN predictions.

The same atmospheric profile developed for June 10 was used for June 7 because of the MFRSR instrument failure at Lunar Lake playa. A sensitivity analysis was performed, which showed that TOA radiance was largely insensitive to changes in the boundary layer surface range when these values exceeded 50 km. TOA radiance varied only a few percent when the surface range was varied between 50 and 150 km. This is due to the high reflectance of the Lunar Lake playa, and low aerosol loading. Since June 7 was very clear (and comparable to June 10), it is very likely that the surface range exceeded 70 km, especially since it exceeded this at nearby Railroad Valley playa as evidenced by the UARSG sun photometer measurements.

The playa surface reflectance at each measurement station was estimated by measuring the soil and a 99 percent reflectance Spectralon® reference panel incorporating Labsphere's Spectralon® hemispherical reflectance calibration curve and modeled Spectralon® panel Bi-directional Reflective Distribution Function (BRDF) effects. The SSC panel BRDF effect was estimated using the Jackson model (Jackson et al., 1992). Reflectance values taken on June 7 and June 10 were used to form spectral albedo files as input into MODTRAN. Once the aerosol estimates and spectral reflectance values were determined, they were combined with the radiosonde profile, site latitude and longitude, satellite acquisition time, and sensor viewing geometry to estimate the TOA radiance. IKONOS spectral response curves were provided by Space Imaging to calculate in-band TOA radiance values. These radiance values were then compared with IKONOS sensor measurements.

Images acquired by IKONOS on June 7 and June 10, 2000 were analyzed to determine the measured radiance values. For each band, DN values along each transect line were averaged and converted to mean radiance values. These mean values were compared to the MODTRAN TOA estimates. Table 2 shows NASA SSC's predicted radiance values compared to Space Imaging's calibrated radiance. The Space Imaging Blue, Green, Red and NIR mean radiances averaged between June 7 and June 10 differ from NASA SSC's modeled radiance by 4 percent, 15 percent, 27 percent, and 49 percent, respectively.

A first order estimate of the error in the TOA radiance estimate is 5 to 7 percent (Biggar et al., 1994) for any single measurement. Additional processing effects not considered in the Biggar paper are now examined. The original NASA SDP IKONOS imagery was ordered with MTFC- On. Additional imagery was ordered with MTFC-Off to assess the effects of this sharpening algorithm. Analysis showed that the RMS difference in the radiance between imagery processed with and without MTFC was less than 2 percent for the spatially uniform Lunar Lake playa. Since averaging along transect lines further reduces the effects of MTFC, MTFC processing effects were ignored in this analysis. The effect of georeferencing interpolation was also ignored for Lunar Lake and other uniform scenes because of the highly uniform nature of the scene and pixel averaging. In addition, any residual effects of compression would be minimized for uniform scenes. Therefore, with approximately a 5 to 7 percent error, the differences between the Space Imaging calibrated radiance and the NASA SSC predicted radiance in the Green, Red, and NIR bands are significant.

7. UARSG Vicarious Characterization

The UARSG performed several independent characterizations of IKONOS radiometry using methods similar to those used in the RSG's work with the Landsat sensors (Thome, 2001). These methods are identical in basic approach to those described above but with some differences in implementation. Solar radiometer data are collected as described above, along with atmospheric pressure and other meteorological variables. An ASD spectroradiometer and 99 percent Spectralon® reference panels were used to provide the reflectance data.

For the UARSG reflectance collection, the user walked a path parallel to the along-track direction of IKONOS for a distance of 80 m. Fifteen of these 80-m lines were walked with the along-track lines separated by 20 m. The site was separated into 60 20-m "pixels" (15 x 4) and ASD data were collected continuously while the user walked the 15 transects. The spectroradiometer was configured to average 20 spectra per sample and 8 samples were collected within a single "pixel." This gave a total of 9,600 spectra collected over the site and 480 samples. It took less than 30 minutes to collect the data when the reference measurements are included. The reference measurements were taken at every 2 transects and at the beginning and end of the collection, giving a total of 9 reference sets, or 72 reference samples.

The reflectance of the site was determined by ratioing the measurements described above to those of the reference panel for which the bi-directional reflectance factor has been determined in the laboratory. The sampling level of the reference, relative to the test site surface, reduces uncertainties due to changes in instrument response with time and changing atmospheric conditions, while keeping the data collection time to a reasonable level. Knowing the BRDF of the reference allows the reflectance of each sample to be computed, taking into account effects

due to sun-angle changes and reflectance panel BRDF over the 30 minutes of data collection. Once each of the spectral samples of the site was converted to reflectance, all 480 data points were averaged to give a single spectral reflectance for the entire site. The same sampling approach and test site size were used for all four sites used by the UARSG.

A critical part of this reflectance retrieval is the characterization of the reference panel in the laboratory. The calibration of this panel was done with reference to a standard made from a pressed polytetrafluoroethylene panel based on a prescribed approach defined by NIST. The calibration reference is a directional-to-hemispheric reflectance standard provided by NIST. Polynomial fits were made to the measured data to calculate the reflectance of the field standard for the sun-view geometry and wavelengths for a given set of field measurements. The Spectralon® sample was calibrated for a nadir viewing sensor with a variety of solar illumination angles. The measurements were made in only one plane, but this does not create problems in the field because the Spectralon® panel was aligned in the field such that the solar incident angle stayed in this same plane. Two different, 18-inch, monolithic Spectralon® panels and two ASD spectroradiometers were used for this work (UARSG serial numbers 6 and 7 for the Spectralon® panels with the number 6 panel paired with ASD687 and the number 7 panel with the ASD614).

Rayleigh scattering, water extinction, ozone, and aerosol distribution were derived from the solar radiometer data and meteorological data. The aerosol distribution was defined in terms of a Junge distribution. These atmospheric and surface data were inputs to a radiative transfer code that computes hyperspectral, at-sensor radiances based on a Gauss-Seidel iteration approach. The code assumes a plane-parallel, homogeneous atmosphere and divides this atmosphere into layers to account for the vertical distribution of scatterers and weak absorption

due to ozone in the visible and near infrared (approximately the 400 to 800-nm spectral range known as the Chappuis absorption band). The Junge parameter described above that was derived from the solar radiometer measurements was used to compute Mie scattering phase functions used in the code. While the radiative transfer code can include non-lambertian effects of the surface, bidirectional reflectance measurements of the surface were not available for this work, so the surfaces were assumed to be lambertian. Past BRDF measurements of the U of A sites and sensitivity analysis indicate that less than a 0.5 percent uncertainty is caused by this assumption.

Strong gaseous absorption effects due to water vapor were determined using MODTRAN, which computes transmittance for the sun-to-surface-to-satellite path for 1-nm intervals from 350 to 2500 nm (Berk et al., 1999). This sun-to-ground-to-sensor transmittance was multiplied by the at-sensor radiance output from the radiative transfer code to correct the radiances for this strong absorption. While this approach is an approximation that excludes interactions between diffusely scattered radiances and absorption, it does not cause large uncertainties for application to IKONOS because of the small effect of absorption within the IKONOS bands and the high surface reflectance of the test sites used in this work.

The relative radiances that are the output of the radiative transfer code were converted to absolute radiance by multiplying by a supplied solar irradiance curve corrected for changes in earth-sun distance. The solar irradiance standard used in this work is that of MODTRAN and is identical to the spectrum selected for NASA's Landsat 7 project. These hyperspectral radiances were then integrated and band-averaged using the supplied spectral response curves from Space Imaging to obtain both the band-integrated and band-averaged spectral radiance at the sensor.

The UARSG performed ground truthing at four different sites. Lunar Lake playa and Railroad Valley playa in Nevada were both imaged twice, and the White Sands Missile Range, New Mexico, and Ivanpah playa, California, were each imaged once. All images used in this analysis were processed with MTFC-On. Table 3 summarizes the UARSG TOA radiance results. The differences between the UARSG vicarious calibration and Space Imaging results are similar to the NASA SSC TOA radiance estimates. The differences between the IKONOS measurement and the predictions based on the ground measurements are greater than 11 percent in the green band, greater than 30 percent in the red band, and greater than 39 percent in the NIR band.

8. SDSU Vicarious Characterization

SDSU performed an IKONOS radiometry characterization in Brookings, South Dakota. The IKONOS sensor collected two images of Brookings, South Dakota, on June 30, 2000. One was a standard original product collected at 17:12 UTC with a collection elevation of 73.12 degrees (collection azimuth of 0.45 degrees) and the other was a precision original product collected one minute later with a collection elevation of 85.59 degrees (collection azimuth of 302.13 degrees). Within the Brookings scene, a 180 m x 180-m uniform grass field (<10 percent variability) was chosen as the ground truth target. Extensive ground truth data were recorded simultaneously with the overpass. This included measurements of surface reflectance, atmospheric transmittance, diffuse-to-global ratio of the hemispherical sky irradiance, and sky path radiance. A radiosonde vertical profile was also acquired at the time of the satellite overpass. The ground truth data were used to calibrate a MODTRAN model predicting the at-sensor total radiance of the target and the sky path radiance.

The reflectance data were taken with an ASD in a manner similar to both NASA SSC and UARSG. There were 108 spectra collected by walking 6 transects over the grass target area, 30 meters apart. Each spectrum was an average of 50 spectral scans recorded in continuous motion to increase spatial averaging. ASD measurements of a Spectralon® panel were also collected to transform the target radiance spectra to reflectance. The panel was calibrated relative to a NIST reflectance standard in the UARSG calibration lab, which included a correction for the BRDF of the panel. Because of greater aerosol loading at this site, a more extensive aerosol estimation technique than described above was used to set up MODTRAN for calculating the TOA radiance. The surface range and aerosol distribution were adjusted to agree with the solar radiometer data recorded at the ground, simultaneous with the IKONOS overpass, and from an aircraft above the boundary layer. Global-to-diffuse irradiance ratios from a Yankee Environmental Systems MFRSR were used to define the scattering phase function asymmetry factor in the MODTRAN calculations. Rayleigh scattering and water vapor absorption were estimated using radiosonde data. In addition, the radiance values derived from the Spectralon® panel measurements were also checked for consistency.

The IKONOS scenes were searched for dark targets that could be assumed to have zero reflectance. A zero reflectance surface will have an at-sensor signal equal to the sky path radiance. For the blue and green bands, these pixels came from shadows in tree strips. For the red and NIR bands, the dark target pixels were from water bodies. MTFC-Off imagery was chosen to avoid any MTFC effects. By extracting, from both scenes, DN's from the target area and surfaces that were identified to have zero reflectance, the gain and bias for transforming at-sensor radiance to image DN's were determined and compared to the gain and bias provided by Space

Imaging. Table 4 summarizes the SDSU TOA radiance estimate results. There is more scatter in this data than the other results due to the more challenging environment (dark target with increased atmospheric contribution), but the results show the same trends as the previous discussions.

9. Compilation of NASA SSC, UARSG and SDSU Results

Each of the three radiance estimates provided by NASA SSC, UARSG, and SDSU were plotted against IKONOS image DN on a single plot for each multispectral band. With each measurement equally weighted, a straight line least squares fit was performed to generate a composite estimate of the gain and offset. The error of this composite measurement should be significantly smaller than the error of each individual measurement. The measurements cover a significant portion of the entire dynamic range of the system. Two forms of least squares fitting, one generating both gain and offset parameters and the other generating only a gain parameter (offset set to zero), were performed. Since very little differences were found between the two approaches and since Space Imaging routinely measures dark counts to subtract the offset, the offset was set to zero and the least squares approach generating only a gain parameter was used.

The composite radiometric calibration curves, along with the Space Imaging calibration curve, are shown in Figure 7. Table 5 lists both the Space Imaging and the NASA team gain coefficients for each of the multispectral bands and the ratio of the two sets of coefficients. Only the Space Imaging IKONOS blue band calibration is in excellent agreement with NASA's composite measurement; the others are significantly different. As a result of this calibration activity, Space Imaging updated their published coefficients to incorporate the NASA team

derived coefficients. Tables 6 through 8 show how the three teams' vicarious calibration TOA radiance estimates compare with the Space Imaging updated calibrated radiance values.

10. MTFC Processing

The effect of MTFC on radiometry for both vicarious calibrations and imagery in general was evaluated as part of this investigation. To facilitate this effort, Space Imaging provided a 5 km x 5-km scene over Phoenix, Arizona with and without MTFC processing. The image contained a large urban area having a high spatial frequency content due to the many edges associated with buildings and roads. There were also some vegetative areas with relatively low spatial frequency content in the image as well. This image was taken on October 12, 1999 at 17:46 UTC. NASA also procured imagery of several of its vicarious calibration sites processed with MTFC-On and MTFC-Off. This paper however highlights the results of the Phoenix scene. First order statistics, means, standard deviations, histograms, Root Mean Squares (RMS) and peak differences between MTFC-On and MTFC-Off imagery were calculated for both the panchromatic and multispectral radiometrically corrected, georeferenced imagery. In addition, all image pairs processed with MTFC-On and MTFC-Off were visually inspected, and the differences between them were displayed visually as a "difference image." MTFC estimates were made, and inverses to these functions were performed to restore compensated imagery back to its MTFC pre-processed state.

A small 1024 x 1024-pixel section from the upper left corner of each original panchromatic and multispectral image was chosen for the analysis. This size image was chosen to enable a quick look and to take advantage of base-two Fast Fourier Transforms (FFTs). A visual inspection of each image pair shows that buildings and other high spatial content objects

are more discernible in the MTFC-processed image. MTFC broadened the histogram on both the low and high DN ends of the MTFC-On image. Some pixels were driven to zero and saturated by the MTFC processing. First order statistics for the two Phoenix images are shown in Tables 9 and 10. The image mean DN value was not affected by MTFC processing. However, the standard deviation between pixels increased by about 10 percent. Cross-sectional plots of the Phoenix MTFC-On and MTFC-Off imagery were made to examine pixel-by-pixel variations. The difference between these plots indicates the magnitude of edge and structure sharpening that has occurred as a result of MTFC. It was not uncommon, in a given row, to observe differences exceeding 50 percent in areas where there were large gradients. The RMS difference in DNs between panchromatic imagery processed with and without MTFC was nearly 8.5 percent and between 4.7 and 7.6 percent for all four multispectral bands.

Differencing the two images, pixel by pixel throughout the scene, generated a difference image. Figure 8 shows the original MTFC-On image and difference image between MTFC-On and MTFC-Off for the Phoenix scene. For display reasons, absolute values of these differences were used. The difference image shows up bright in areas of many edges due to buildings and roads, indicating large differences between the imagery processed with and without MTFC in those areas. The difference image shows up darker in more uniform areas, indicating smaller differences between the two images in those regions.

The MTFC function was estimated in the frequency domain by calculating the ratio of the Fourier transform of the MTFC processed image to the Fourier transform of the non-MTFC processed image. To improve the estimate of the transfer function, the image was broken down into sixteen 256 x 256-point transforms, which were averaged to estimate the MTFC function for

each small section of the image. The panchromatic MTFC function appeared to be a flower petal in shape, indicating relative symmetry between the in-track and cross-track directions. The multispectral MTFC functions appeared to be more cylindrical in shape and boosted the high spatial frequencies by half as much as in the panchromatic case. Additionally, the cross-track direction is more strongly compensated than the in-track direction. Similar results were obtained for each multispectral band, but in general the effects of MTFC increased in going from the blue to NIR band. Contour plots of the two dimensional MTFC functions show that they have been rotated relative to the image coordinate system. This appears to be due to geometric referencing. Space Imaging performs the MTFC and georeferencing simultaneously with a combined convolution kernel.

To test the validity of the estimated MTFC function, a 256 x 256-pixel MTFC-processed image provided by Space Imaging was processed again with the inverse of the MTFC function estimate. Before the MTFC function estimate was inversed, it was further smoothed with a 5 x 5 convolution kernel-averaging filter. If a good estimate of the MTFC function was found, the resulting restored image should be close to the original image that was not MTFC processed. The RMS difference between imagery that was not processed with MTFC and imagery that had been restored back to its pre-MTFC processed state was less than 1 percent. Applying the same inverse function to other images did not always produce ideal results. This indicates the MTFC process is partially reversible due to the fact that georeferencing is done at the same time that MTFC processing occurs.

Another interesting observation is that the SNR is lowered with MTFC processing. Simulated scenes representing shot noise limited imagery show a significant increase

in noise (20-40 percent) for MTFC processed multispectral imagery with respect to non-MTFC-processed imagery. This is not surprising since the shot noise process will manifest itself as a two-dimensional white noise process that will have significant high spatial frequency components which will be amplified when MTFC is applied. This increased noise is evident in both simulated and acquired scenes containing known uniform areas. This likely explains why acquired scenes such as Lunar Lake show nearly a 2 percent RMS difference in pixel values between MTFC-Off and MTFC-On imagery in the NIR band. Simulations over ideal uniform scenes, which do not contain noise, show no difference in pixel value between MTFC-Off and MTFC-On imagery.

11. Summary

NASA performed a relative radiometric accuracy assessment of IKONOS imagery using large uniform Antarctic and Saharan scenes and found that differences between detector arrays were well within the Space Imaging data specification. Uniform scenes for this analysis were found in part by searching through the EarthSat Landsat 5 TM imagery purchased through the NASA SDP. The relative radiometric accuracy assessment was conducted by comparing values obtained by summing the pixels of a uniform image in the column direction. This method, which amplifies detector defect effects, found that differences between summed pixels were less than 1.5 percent. This analysis illustrates that Space Imaging has properly calibrated the detectors in a relative sense, and that a single calibration coefficient can be used to calibrate the entire image.

The first independent absolute radiometric characterization of a new class of commercial imagery was conducted. Several different vicarious calibrations from three different teams (NASA SSC, the UARSG, and SDSU) were combined to assess the IKONOS radiometric

performance. Although each team used unique radiative transfer methods and slightly different approaches, the results were in excellent agreement. In the green, red and NIR bands, discrepancies ranging from 21 percent to 82 percent were found between the vicarious calibration and Space Imaging calibration. As a result of this activity, Space Imaging updated their IKONOS multispectral radiometric calibration coefficients. This NASA team is continuing to perform vicarious calibrations to ascertain radiometric stability of the IKONOS system.

A first look at the question "Should MTFC be applied to imagery procured under the NASA Scientific Data Purchase (SDP)?" was taken. At this stage, it is recommended that MTFC be applied to the imagery when the imagery will be used primarily to inspect features visually. Over relatively uniform scenes such as vegetative areas, little difference was observed with either option. In scenes with many edges and point sources, individual pixel values were observed to differ by more than 50 percent between the two options with scene RMS differences typically less than 8.5 percent for both the panchromatic and multispectral products. In these cases and when radiometry is important, imagery without MTFC processing is preferable.

Future work will examine additional imagery with and without MTFC, as well as imagery georeferenced with nearest neighbor and cubic convolution interpolation to determine how these types of processing effect classifiers and absolute radiometric accuracy. Uniform scenes are being procured to examine the SNR of MTFC-On and MTFC-Off imagery, as well as relative radiometry.

Acknowledgments

This work was supported by the NASA Earth Science Applications Directorate under contract number NAS 13-650 at the John C. Stennis Space Center, Mississippi.

References

Bauer, M., Sawaya K., 2001. Extending Satellite Remote Sensing to Local Scales: Minnesota Experience with IKONOS Data. Proceedings of NASA/NIMA/USGS High Spatial Resolution Commercial Imagery Workshop, March 19-22. Greenbelt, Maryland, CD-ROM.

Berk A., Anderson, G. P., Acharya, P. K., Chetwynd, J. H., Bernstein, L. S., Shettle, E. P., Matthew, M. W., Adler-Golden, S. M., 1999. MODTRAN4 Users Manual, Air Force Research Laboratory, Space Vehicles Directorate, Air Force Materiel Command, Hanscom AFB, Massachusetts.

Biggar, S. F., Slater, P. N., Gellman, D. I., 1994. Uncertainties in the In-Flight Calibration of Sensors with Reference to Measured Ground Sites in the 0.4-1.1 μm Range. Remote Sensing Environment, 48: 245-252.

Brower, B.V., Cosgrove, M.A., Lewis, D.H., VanLare, G.R., Fisher, T.J., Charneski, D.M., 2000. An Advanced Space-qualified Downlink Image Compression ASIC for Commercial Remote Sensing Applications. Proc. SPIE 2000, 4115: 277-786.

DaMommio, T., Kuo, S., 1993. Optical Design for the ATLAS Multispectral Scanner, NASA Stennis Space Center, Mississippi.

Dinguirard, M., Slater, P. N., 1999. Calibration of Space-Multispectral Imaging Sensors: A Review. Remote Sensing of the Environment, 68: 194-205.

Ehsani, A. R., Reagan, J. A., and Erxleben, W. H., 1998. Design and Performance Analysis of an Automated 10-channel Solar Radiometer Instrument. Journal of Atmospheric and Oceanic Technology, 15: 697-707.

Hilbert K., Pagnutti, M., Ryan, R., Zanoni, V., 2002. (Draft) Detecting Uniform Areas For Vicarious Calibration Using Landsat TM Imagery: A Study Using The Arabian And Saharan Deserts. Remote Sensing of Environment.

Holst, G., 1995. Electro-Optical Imaging Performance, pp. 146-147, SPIE Optical Engineering Press, Bellingham, Washington

Jackson, R. D., Clarke, T. R., Moran, M. S., 1992, Bidirectional Calibration Results for 11 Spectralon and 16 $BaSO_4$ Reference Reflectance Panels. Remote Sensing of Environment, 40: 231-239.

Justice, C., Eck, T., Tanré, D., Holben, B., 1991. The Effect of Water Vapor on the Normalized Difference Vegetation Index derived for the Sahelian Region from NOAA AVHRR Data. International Journal of Remote Sensing, Vol. 12, No. 6: 1165-1187.

Kaufman, Y. J., Holben, B. N., 1993. Calibration of the AVHRR Visible and Near-IR Bands by Atmospheric Scattering, Ocean Glint and Desert Reflection. International Journal of Remote Sensing, Vol. 14, No. 1: 21-52.

Leachtenauer, J., Malila, W., Irvine, J., Colburn, L., Salvaggio, N., 1997. General Image Quality Equation: GIQE. Applied Optics, 36: 8322-8328.

Meygret, A., Briottet, X., Henry, P., Hagolle, O., 2000. Calibration of SPOT4 HRVIR and VEGETATION cameras over the Rayleigh scattering. Proceedings SPIE, 4135: 302-313.

NASA Commercial Remote Sensing Program Office, 2001. Proceedings of NASA/NIMA/ USGS High Spatial Resolution Commercial Imagery Workshop, March 19-22, Greenbelt, Maryland, CD-ROM.

NASA Earth Science Applications Directorate, 2002. Proceedings of NASA/NIMA/USGS High Spatial Resolution Commercial Imagery Workshop, March 25-27, Reston, Virginia, CD-ROM.

NASA Earth Science Applications Directorate, 2002. Scientific Data Purchase Bibliography (compiled by L. Underwood), April 11, Stennis Space Center, Mississippi.

Slater, P. N., Biggar, S. F., Holm, R. G., Jackson, R. D., Mao, Y., Moran, M. S., Plamer, J. M., Yuan, B., 1987. Reflectance- and Radiance-Based Methods for the In-Flight Absolute Calibration of Multispectral Sensors. Remote Sensing of Environment, 22: 11-37.

Slater, P. N., Biggar, S. F., Thome, K. J., Gellman, D. I., Spyak, P. R., 1994. The In-Flight Radiometric Calibration of ASTER by Reference to Well-Characterized Scenes. SPIE, Platforms and Systems 2317: 49-60.

Slater, P.N., Biggar, S.F., Thome, K. J., Gellman, D. I., and Spyak, P. R., 1996. Vicarious Radiometric Calibration of EOS Sensors. Journal of Atmospheric and Oceanic Technology, 13: 349-359.

Thome, K. J., Gellman, D. I., Parada, R. J., Biggar, S. F., Slater, P. N., and Moran, M.S., 1993. In-Flight Radiometric Calibration of Landsat-5 Thematic Mapper from 1984 to Present. Proc. SPIE 1938: 126-130.

Thome, K. J., 2001. Absolute Radiometric Calibration of Landsat-7 ETM+ using the Reflectance-based Method. Remote Sensing of Environment, 78: 27-38.

Tables

Table 1. Vicarious Calibration Acquisition Summary

Date	Location	Overpass Time (UTC)	Solar Zenith (deg)	Solar Azimuth (deg)	Sensor Nadir (deg)	Sensor Azimuth (deg)	Nominal GSD (m)
5/26/00	WSMR NM	17:38	21.9	116.9	12.1	346	0.85
6/7/00	Lunar Lake NV	18:16	24.5	123.2	19.0	158	0.90
6/7/00	RRV NV	18:14	24.3	123.8	11.6	144	0.85
6/10/00	Lunar Lake NV	18:23	22.9	126.3	17.0	351	0.89
6/10/00	RRV NV	18:23	22.8	126.9	9.5	267	0.84
7/21/00	Ivanpah CA	18:20	24.5	122.6	6.4	284	0.83
6/30/00	Brookings SD	17:12	26.5	136.1	17.9	0.45	0.87
6/30/00	Brookings SD	17:13	25.8	135.9	4.4	302	0.83

Table 2. NASA SSC TOA Radiance Results

Site	Date	Band	DN	TOA Radiance [W/(m^{2}sr)]	IKONOS Radiance [W/(m^{2}sr)]	% Difference
Lunar Lake	6/7/00	Blue	828	12.56	12.991	-3.43
		Green	1178	16.987	20.551	-20.98
		Red	1174	13.531	17.711	-30.89
		NIR	1083	14.153	21.536	-52.17
Lunar Lake	6/10/00	Blue	811	12.841	12.029	6.32
		Green	1093	17.28	19.075	-10.39
		Red	1108	13.642	16.712	-22.50
		NIR	1028	14.053	20.442	-45.46

Table 3. UARSG Results for Playa, White Sands Missile Range and Ivanpah

Site	Date	Band	DN	TOA Radiance [W/(m2sr)]	IKONOS Radiance [W/(m2sr)]	% Difference
Lunar Lake	6/7/00	Blue	851	13.155	13.359	-1.56
		Green	1216	18.287	21.222	-16.05
		Red	1216	13.509	18.341	-35.77
		NIR	1123	15.293	22.326	-45.99
Lunar Lake	6/10/00	Blue	791	12.884	12.418	3.62
		Green	1137	17.738	19.843	-11.87
		Red	1151	13.272	17.360	-30.81
		NIR	1062	15.140	21.113	-39.45
Railroad	6/7/00	Blue	734	9.953	11.523	-15.77
Valley		Green	1012	13.431	17.661	-31.49
		Red	968	9.258	14.600	-57.70
		NIR	875	10.513	17.400	-65.47
Railroad	6/10/00	Blue	667	10.352	10.471	-1.14
Valley		Green	914	13.990	15.951	-14.02
		Red	876	9.718	13.212	-35.95
		NIR	787	11.009	15.646	-42.12
WSMR	5/26/00	Blue	1422	22.160	22.323	-0.74
		Green	1826	28.236	31.867	-12.86
		Red	1694	18.641	25.551	-37.07
		NIR	1564	20.749	31.093	-49.85
Ivanpah	7/21/00	Blue	642	9.668	10.078	-4.24
		Green	935	13.946	16.318	-17.01
		Red	999	10.956	15.068	-37.53
		NIR	929	12.745	18.469	-44.91

Table 4. SDSU TOA Radiance Results

Site	Date	Band	DN	TOA Radiance [W/(m2sr)]	IKONOS Radiance [W/(m2sr)]	% Difference
Brookings	6/30/00	Blue	249	3.618	3.910	-8.04
Grass	Pass 1	Green	289	4.168	5.044	-21.01
Pixels		Red	225	2.7	3.394	-25.69
		NIR	577	7.72	11.471	-48-59
Brookings	6/30/00	Blue	184	2.439	2.889	-18.43
Dark Pixels	Pass 1	Green	149	1.806	2.600	-43.98
		Red	71	0.652	1.071	-64.25
		NIR	60	0.654	1.193	-82.39
Brookings	6/30/00	Blue	261	3.679	4.097	-11.37
Grass	Pass 2	Green	304	4.219	5.305	-25.75
Pixels		Red	239	2.718	3.605	-32.63
		NIR	589	7.741	11.710	-51.27
Brookings	6/30/00	Blue	186	2.488	2.920	-17.36
Dark Pixels	Pass 2	Green	147	1.839	2.566	-39.50
		Red	70	0.660	1.056	-59.97
		NIR	40	0.651	0.795	-22.15

Table 5. NASA Team Gain Coefficients

Band	Space Imaging Gain	NASA Team Gain	(NASA Team)/(SI Gain)
Blue	63.7	64.1 +/- 2.6	1.01
Green	57.3	65.4 +/- 2.7	1.14
Red	66.3	87.7 +/- 3.1	1.32
NIR	50.3	75.8 +/- 2.9	1.51

Table 6. NASA SSC TOA Radiance Results Using Updated SI Calibration Coefficients

Site	Date	Band	DN	TOA Radiance [W/(m2sr)]	IKONOS Radiance [W/(m2sr)]	% Difference
Lunar Lake	6/7/00	Blue	828	12.56	13.081	-4.148
		Green	1178	16.987	18.151	-6.852
		Red	1174	13.531	13.976	-3.289
		NIR	1083	14.153	14.517	-2.572
Lunar Lake	6/10/00	Blue	811	12.841	12.812	0.226
		Green	1093	17.28	16.841	2.541
		Red	1108	13.642	13.19	3.313
		NIR	1028	14.053	13.78	1.943

Table 7. UARSG TOA Radiance Results Using Updated SI Calibration Coefficients

Site	Date	Band	DN	TOA Radiance [W/(m^{2}sr)]	IKONOS Radiance [W/(m^{2}sr)]	% Difference
Lunar Lake	6/7/00	Blue	851	13.155	13.444	-2.20
		Green	1216	18.287	18.737	-2.46
		Red	1216	13.509	14.476	-7.16
		NIR	1123	15.293	15.054	1.57
Lunar Lake	6/10/00	Blue	791	12.884	12.496	3.01
		Green	1137	17.738	17.519	1.23
		Red	1151	13.272	13.702	-3.24
		NIR	1062	15.14	14.236	5.97
Railroad	6/7/00	Blue	734	9.953	11.596	-16.50
Valley		Green	1012	13.431	15.593	-16.10
		Red	968	9.258	11.524	-24.47
		NIR	875	10.513	11.729	-11.57
Railroad	6/10/00	Blue	667	10.352	10.537	-1.79
Valley		Green	914	13.99	14.083	-0.67
		Red	876	9.718	10.429	-7.31
		NIR	787	11.009	10.550	4.17
WSMR	5/26/00	Blue	1422	22.16	22.464	-1.37
		Green	1826	28.236	28.136	0.36
		Red	1694	18.641	20.167	-8.18
		NIR	1564	20.749	20.965	-1.04
Ivanpah	7/21/00	Blue	642	9.668	10.142	-4.90
		Green	935	13.946	14.407	-3.31
		Red	999	10.956	11.893	-8.55
		NIR	929	12.745	12.453	2.29

Table 8. SDSU TOA Radiance Results Using Updated SI Calibration Coefficients

Site	Date	Band	DN	TOA Radiance [W/(m^{2}sr)]	IKONOS Radiance [W/(m^{2}sr)]	% Difference
Brookings	6/30/00	Blue	249	3.618	3.934	-8.72
Grass	Pass 1	Green	289	4.168	4.453	-6.84
Pixels		Red	225	2.7	2.679	0.79
		NIR	577	7.72	7.735	-0.19
Brookings	6/30/00	Blue	184	2.439	2.907	-19.18
Dark Pixels	Pass 1	Green	149	1.806	2.296	-27.12
		Red	71	0.652	0.845	-29.64
		NIR	60	0.654	0.804	-22.98
Brookings	6/30/00	Blue	261	3.679	4.123	-12.07
Grass	Pass 2	Green	304	4.219	4.684	-11.02
Pixels		Red	239	2.718	2.845	-4.68
		NIR	589	7.741	7.895	-2.00
Brookings	6/30/00	Blue	186	2.488	2.938	-18.10
Dark Pixels	Pass 2	Green	147	1.839	2.265	-23.17
		Red	70	0.66	0.833	-26.26
		NIR	40	0.651	0.536	17.64

Table 9. First-order Panchromatic Statistics Summary of Phoenix Site

Statistic	Panchromatic MTFC Off	Panchromatic MTFC On
Mean DN	598.2	598.2
Standard Dev DN	183.6	205.2
Min DN	149	0
Max DN	1983	2047
Max Diff DN	844	
Min Diff DN	-781	
RMS Difference DN	.085	

Table 10. First-order Multispectral Statistics Summary of Phoenix Site

	Blue		Green		Red		NIR	
	MTFC Off	MTFC On	MTFC Off	MTFC On	MTFC Off	MTFC On	MTFC Off	MTFC On
Mean DN	328.3	328.3	412.5	412.5	397.8	397.8	426.9	426.8
Std Dev DN	89.46	97.89	133.45	147.29	146.0	161.5	126.2	145.84
Min DN	153	0	135	0	83	0	65	0
Max DN	2047	2047	2047	2047	2047	2047	2047	2047
Max Diff DN	425		444		454		427	
Min Diff DN	-327		-307		-327		-378	
RMS Difference DN	.047		.059		.070		.0761	

Figure Captions

Figure 1. IKONOS Spectral Response Curves for Panchromatic and Multispectral Bands

Figure 2. IKONOS Blue Band of the Uniform Saharan Scene (Stretched)

Figure 3. Cross sectional plot of Pixels Summed in the In-track Direction of the Uniform Saharan Scene.

Figure 4. IKONOS Image of Lunar Lake Playa acquired on June 7, 2000

Figure 5. IKONOS Lunar Lake Acquisition Geometry

Figure 6. Comparison of Solar Radiometer Measurements and MODTRAN Prediction for June 10, 2000

Figure 7. NASA Team Radiometric Compilation Calibration Curves

Figure 8. Phoenix NIR MTFC-On Image (top) and Difference Between MTFC-On and MTFC-Off NIR Imagery (bottom).

Figures

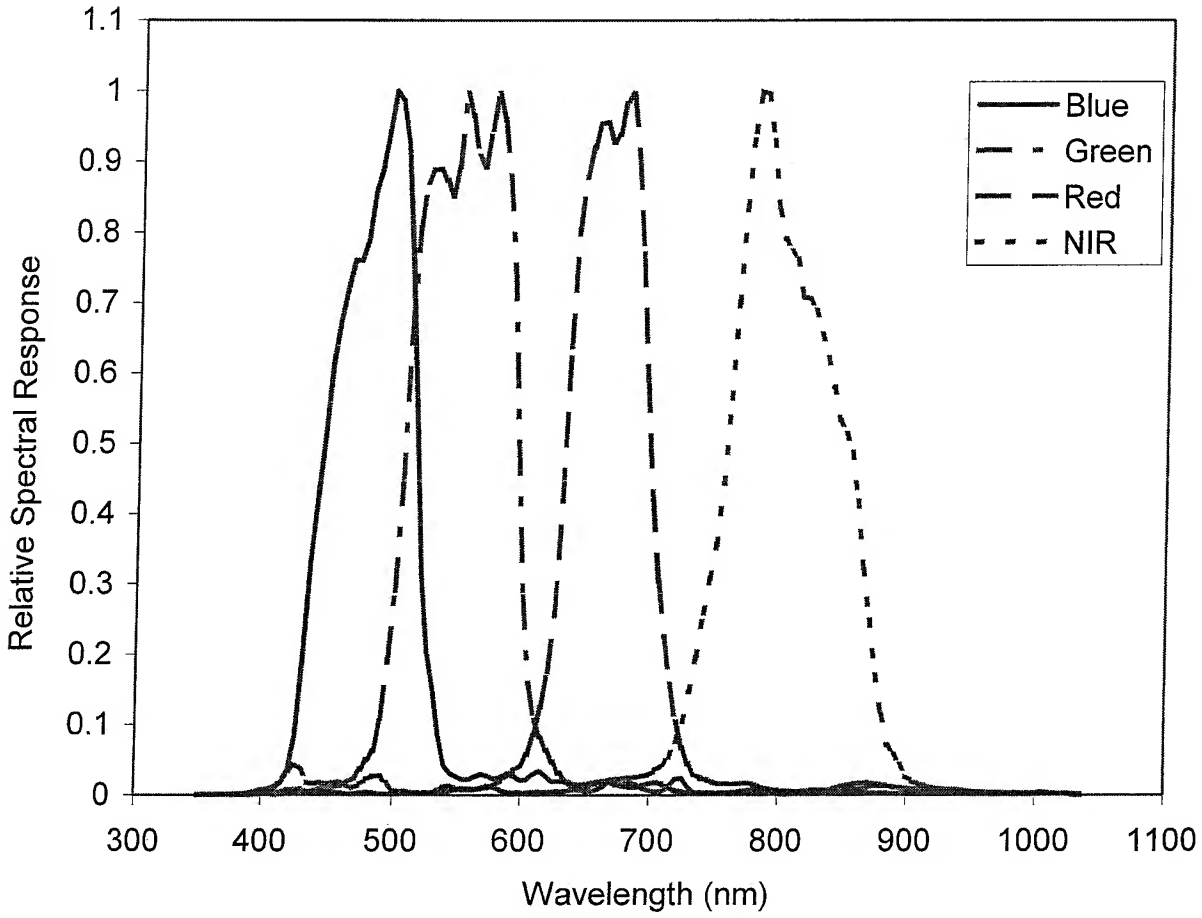

Figure 1

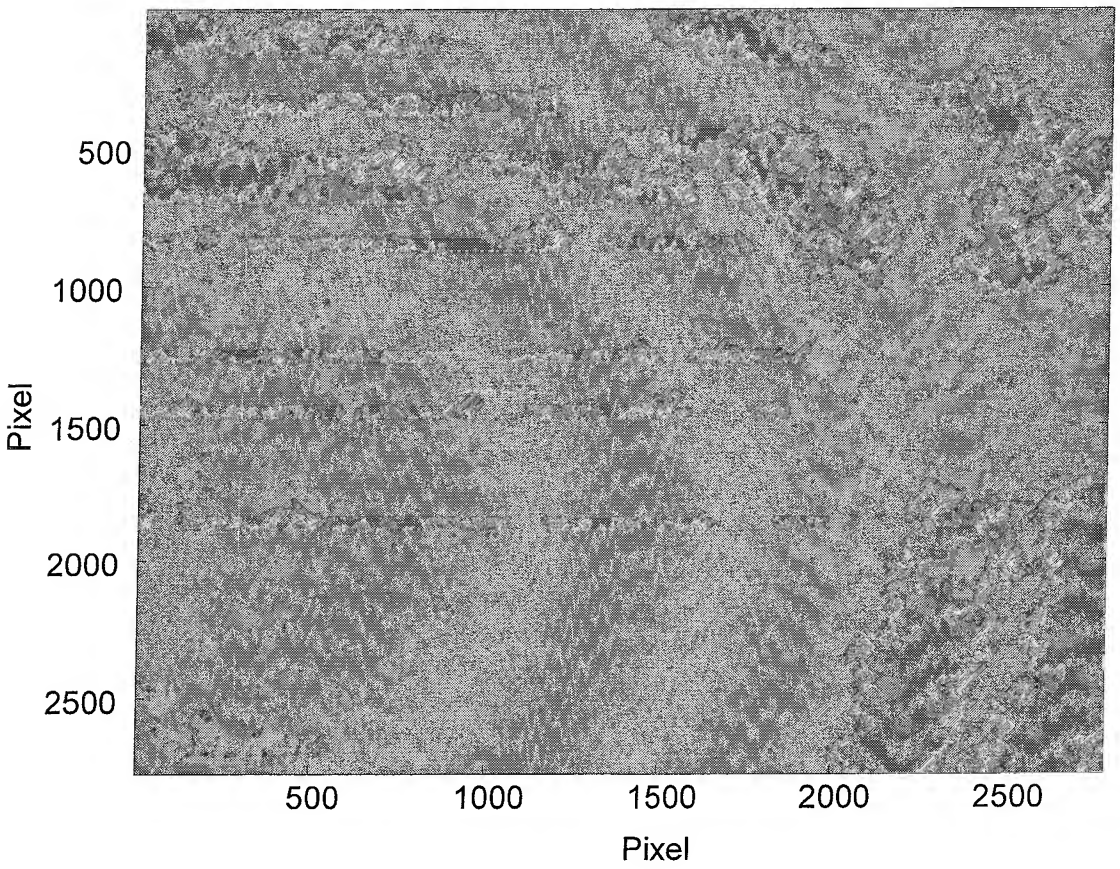

Figure 2

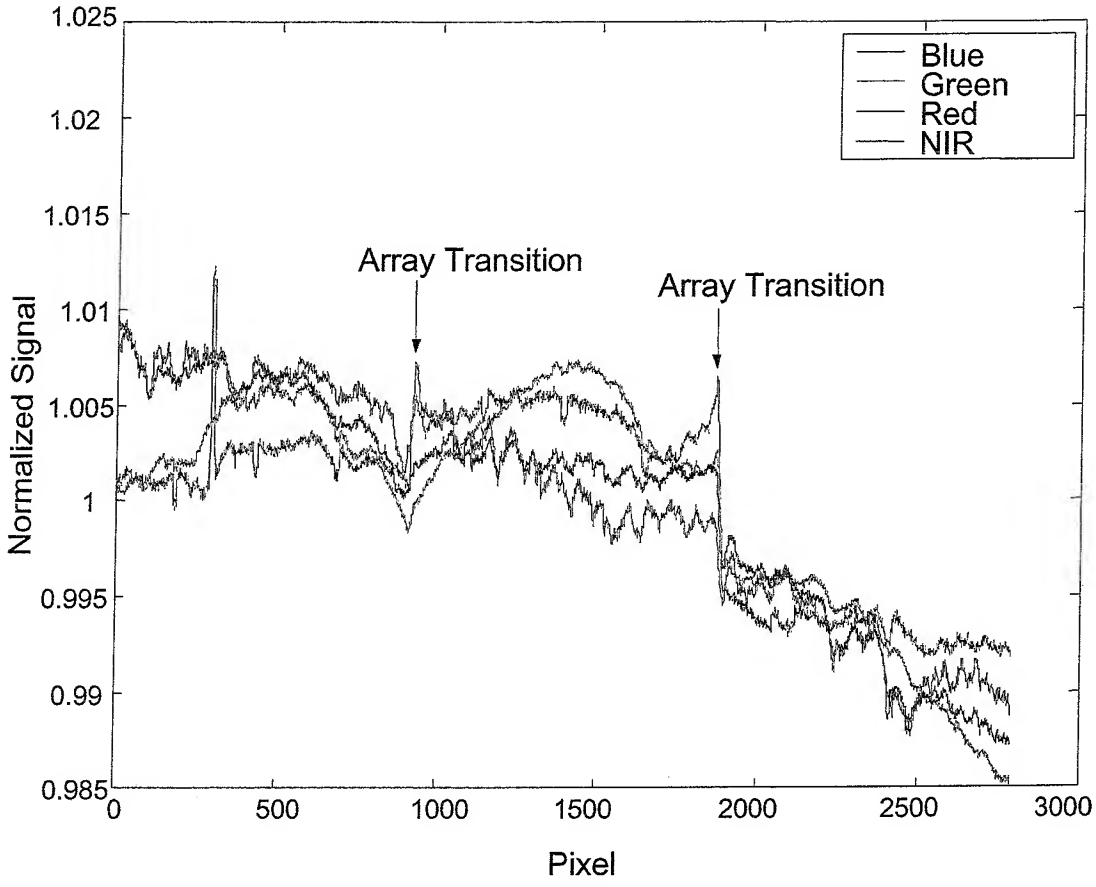
Blue
Green
Red
NIR
Array Transition
Array Transition
Normalized Signal
Pixel
1.025
1.02
1.015
1.01
1.005
1
0.995
0.99
0.985
0
500
1000
1500
2000
2500
3000

Figure 3

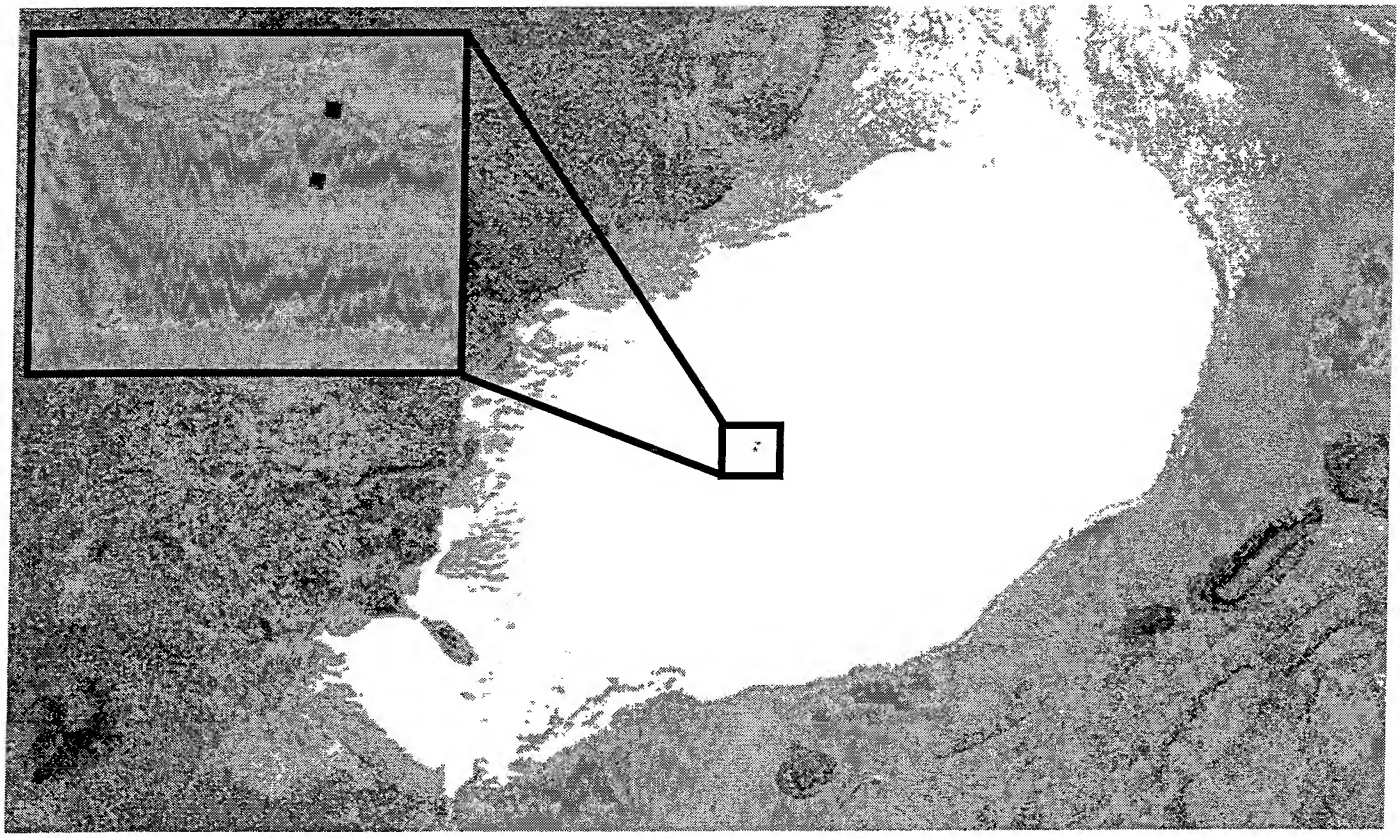

Figure 4

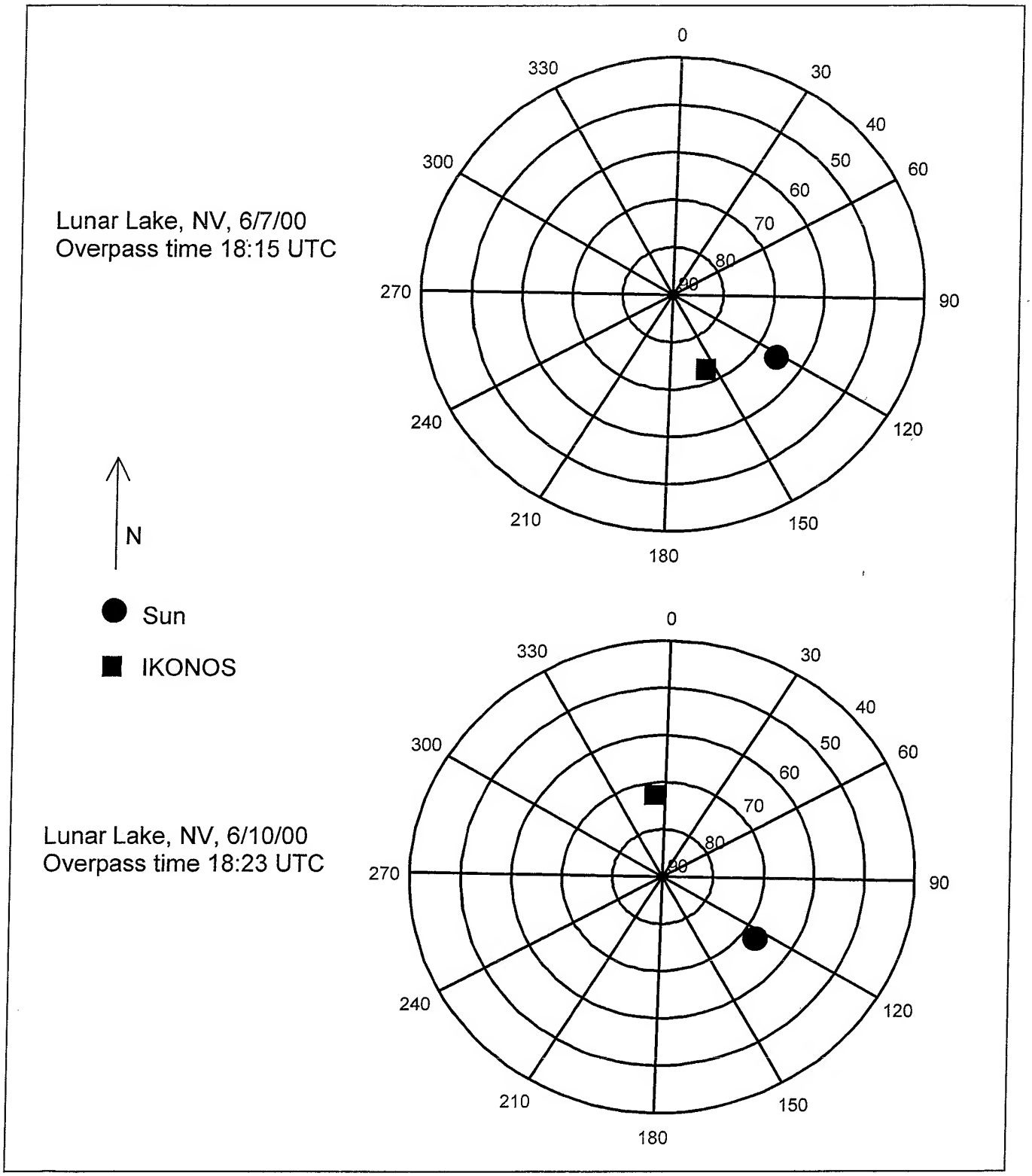
Lunar Lake, NV, 6/7/00
Overpass time 18:15 UTC
0
30
40
50
60
70
80
90
120
150
180
210
240
270
300
330
N
Sun
IKONOS
Lunar Lake, NV, 6/10/00
Overpass time 18:23 UTC

Figure 5

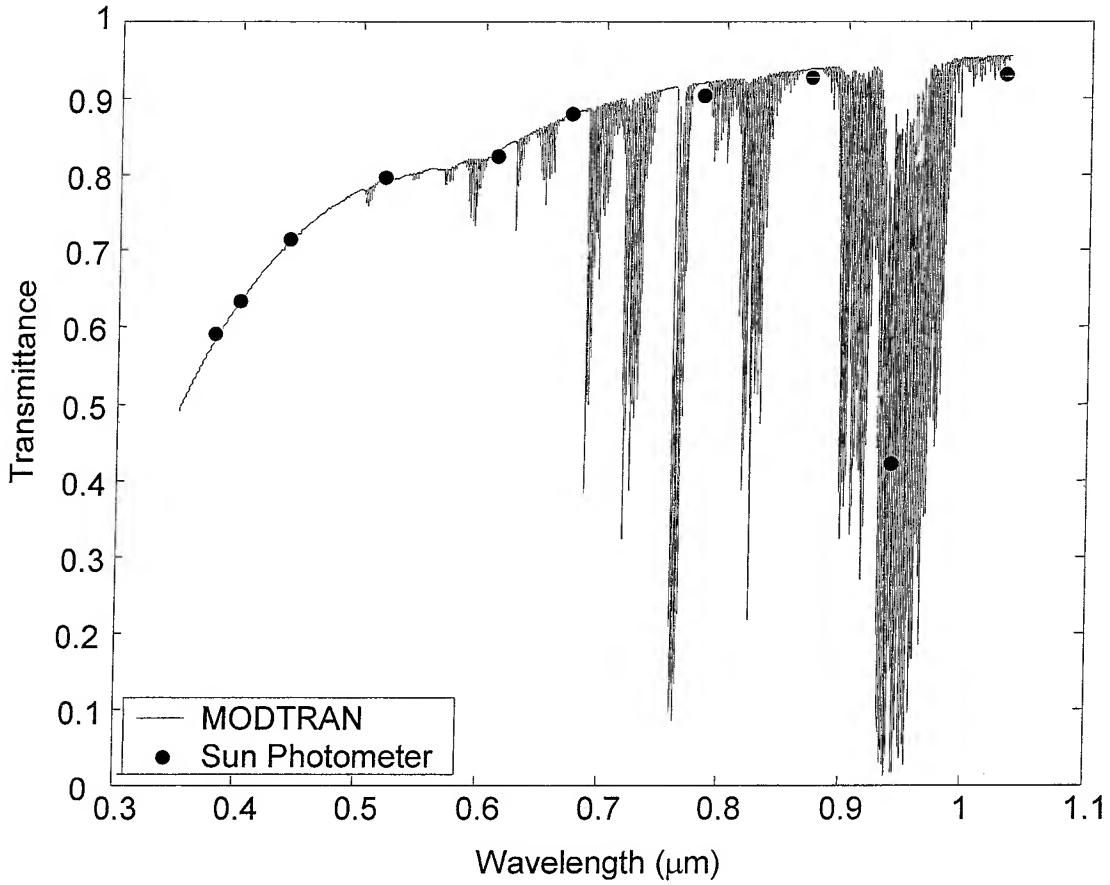
Transmittance
Wavelength (μm)
MODTRAN
Sun Photometer
0
0.1
0.2
0.3
0.4
0.5
0.6
0.7
0.8
0.9
1
0.3
0.4
0.5
0.6
0.7
0.8
0.9
1
1.1

Figure 6

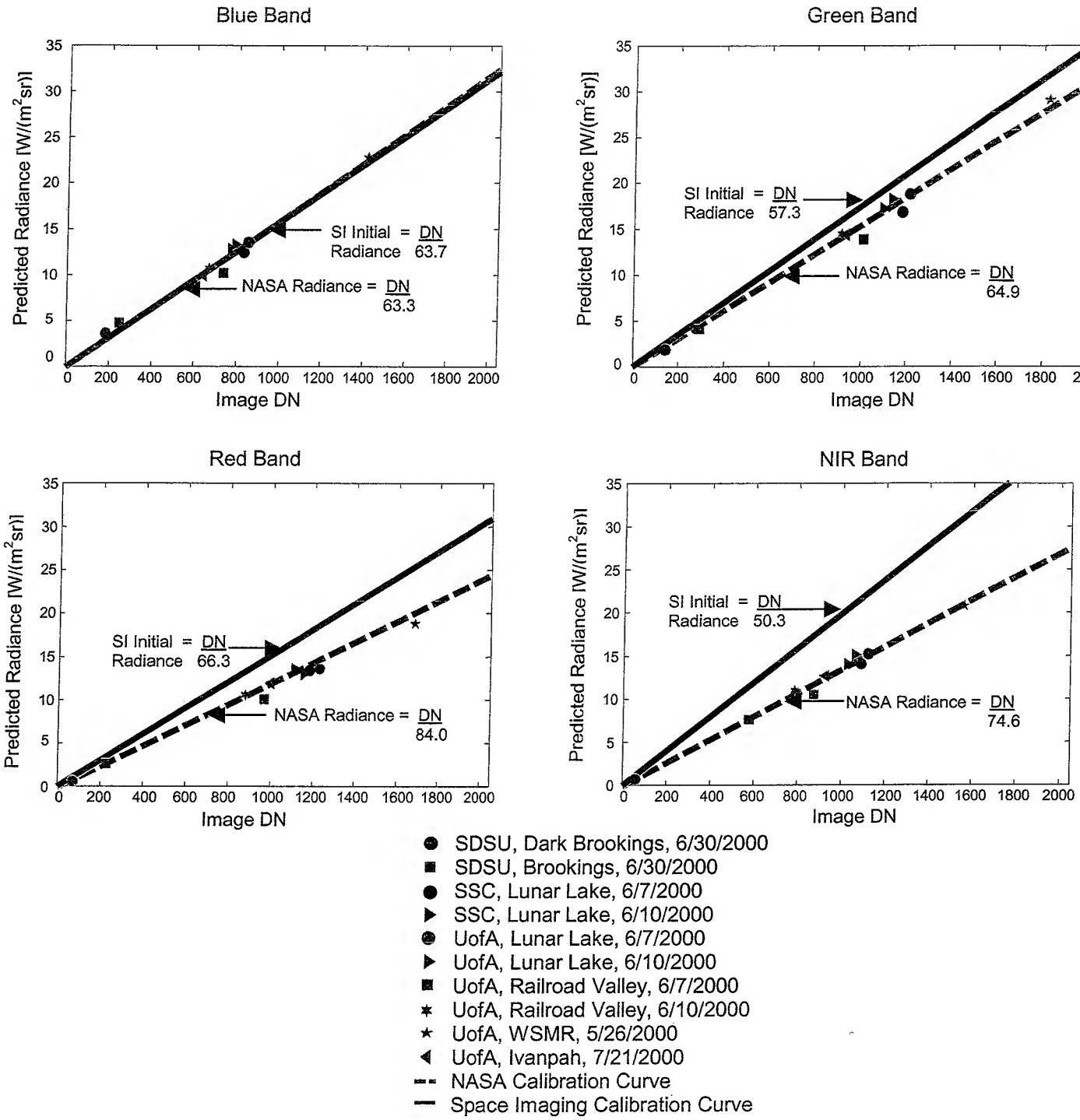
Blue Band
Green Band
Red Band
NIR Band
Predicted Radiance [W/(m²sr)]
Image DN
SI Initial = DN
Radiance 63.7
NASA Radiance = DN
63.3
SI Initial = DN
Radiance 57.3
NASA Radiance = DN
64.9
SI Initial = DN
Radiance 66.3
NASA Radiance = DN
84.0
SI Initial = DN
Radiance 50.3
NASA Radiance = DN
74.6
SDSU, Dark Brookings, 6/30/2000
SDSU, Brookings, 6/30/2000
SSC, Lunar Lake, 6/7/2000
SSC, Lunar Lake, 6/10/2000
UofA, Lunar Lake, 6/7/2000
UofA, Lunar Lake, 6/10/2000
UofA, Railroad Valley, 6/7/2000
UofA, Railroad Valley, 6/10/2000
UofA, WSMR, 5/26/2000
UofA, Ivanpah, 7/21/2000
NASA Calibration Curve
Space Imaging Calibration Curve

Figure 7

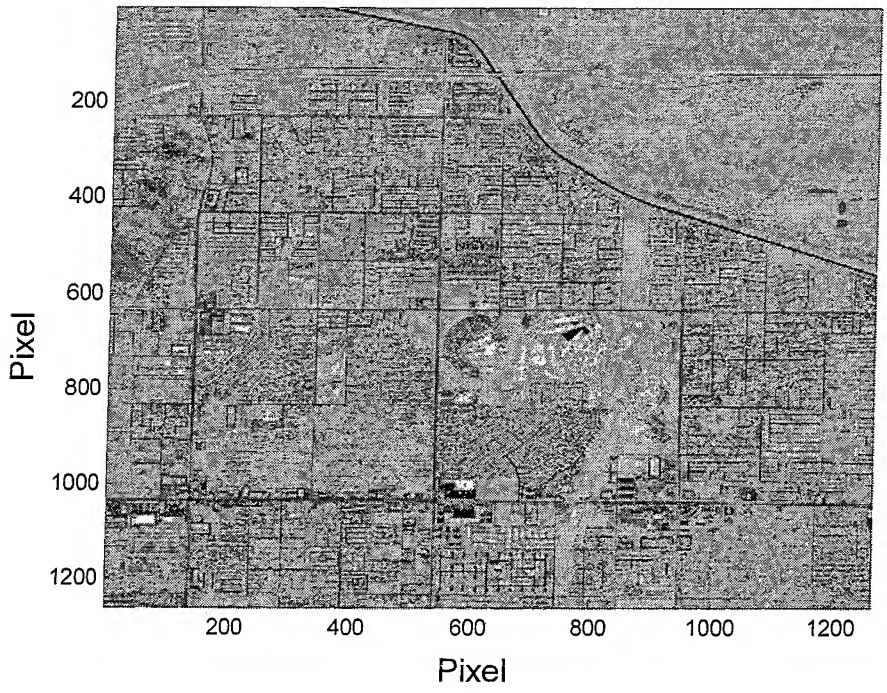
200
400
600
800
1000
1200
Pixel
200
400
600
800
1000
1200
Pixel

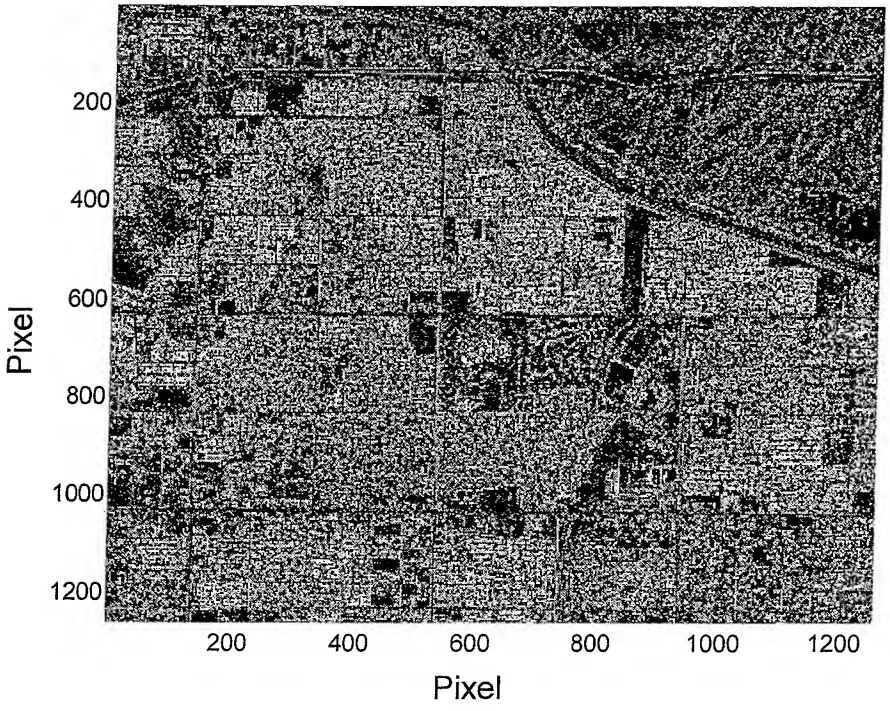
200
400
600
800
1000
1200
Pixel
200
400
600
800
1000
1200
Pixel

Figure 8

REPORT DOCUMENTATION PAGE

Form Approved
OMB No. 0704-0188

1. REPORT DATE *(DD-MM-YYYY)*	2. REPORT TYPE	3. DATES COVERED *(From - To)*
12-08-2002		

4. TITLE AND SUBTITLE
Radiometric Characterizaiton of IKONOS Multispectral Imagery

5a. CONTRACT NUMBER
NAS13-650

5b. GRANT NUMBER

5c. PROGRAM ELEMENT NUMBER

6. AUTHOR(S)
Mary Pagnutti Stephen Schiller
Robert Ryan
Michelle Delly
Kara holecamp
Vicki Zanoni
Kurtis Thome

5d. PROJECT NUMBER

5e. TASK NUMBER

5f. WORK UNIT NUMBER

7. PERFORMING ORGANIZATION NAME(S) AND ADDRESS(ES)
LMSO - Stennis Programs

8. PERFORMING ORGANIZATION REPORT NUMBER
SE-2002-08-00057-SSC

9. SPONSORING/MONITORING AGENCY NAME(S) AND ADDRESS(ES)
Earth Science Applicaitons Directorate

10. SPONSORING/MONITOR'S ACRONYM(S)

11. SPONSORING/MONITORING REPORT NUMBER

12. DISTRIBUTION/AVAILABILITY STATEMENT
Publicly Available STI per form 1676

13. SUPPLEMENTARY NOTES
Periodical Remote Sensing of Environment

14. ABSTRACT

A radiometric characterization of Space Imaging's IKONOS 4-m multispectral imagery has been performed by a NASA funded team from the John C Stennis Space Center, the University of Arizona Remote Sensing Group and South Dakota State University. Both intrinsic radiometry and the effects of Space Imaging processing on radiometry were investigated. Relative radiometry was examined with uniform Antarctic and Saharan sites. Absolute radiometric calibration was perfomred using reflectance-based vicarious calibration methods on several unifom sites imaged by IKONOS, coincident with ground-based surface and atmospheric measurements. Ground based data and the IKONOS spectral response funtion served as input to radiative transfer codes to generate a Top-of-Atmosphere radiance estimate. Calibraiton coefficients derived from each vicarious calibration were combined to generate an IKONOS radiometric gain coefficient for each multispectral band assuming a linear response over the full dynami c range of the instrument. These calibration coeffieciemts were made available to Space Imaging, which subsequently adopted them by updating its inintial set of calibration coeffiecients. IKONOS imagery procured through the NASA Scientific Data Purchase program is processed

15. SUBJECT TERMS

16. SECURITY CLASSIFICATION OF:			17. LIMITATION OF ABSTRACT	18. NUMBER OF PAGES	19b. NAME OF RESPONSIBLE PERSON
a. REPORT	b. ABSTRACT	c. THIS PAGE			Mary Pagnutti
					19b. TELEPHONE NUMBER *(Include area code)*
U	U	U	UU	48	(228) 688-2135